THE JOURNAL OF PHYSICAL CHEMISTRY C
A JOURNAL OF THE AMERICAN CHEMICAL SOCIETY

pubs.acs.org/JPCC

Article

Direct Observation of Reactant, Intermediate, and Product Species for Nitrogen Oxide-Selective Catalytic Reduction on Cu-SSZ-13 Using *In Situ* Soft X-ray Spectroscopy

Linsey C. Seitz,* Dmitry E. Doronkin, Dirk Hauschild, Maria Casapu, Deniz Zengel, Anna Zimina, Dagmar Kreikemeyer-Lorenzo, Monika Blum, Wanli Yang, Jan-Dierk Grunwaldt, Clemens Heske, and Lothar Weinhardt*

Cite This: *J. Phys. Chem. C* 2022, 126, 20998–21009

Read Online

ACCESS | Metrics & More | Article Recommendations | Supporting Information

ABSTRACT: Catalytic processes have supported the development of myriad beneficial technologies, yet our fundamental understanding of the complex interactions between reaction intermediates and catalyst surfaces is still largely undefined for many reactions. Experimental analyses have generally been limited to investigation of catalyst materials or a subset of functional groups as indirect probes of the critical surface-bound intermediate species and reaction mechanisms. A more direct approach is to probe the intermediate species themselves, but this requires direct study of the local chemical environment of light elements. In this work, we use soft X-ray emission spectroscopy (XES) and a custom-designed *in situ* reactor cell to directly observe and characterize the electronic structure of reactant, intermediate, and product species under reaction conditions. Specifically, we employ N K XES to probe the interaction of various nitrogen species with a Cu-SSZ-13 catalyst during selective catalytic reduction of nitrogen oxides (NO and NO_2) by ammonia (NH_3-SCR), a reaction that is critical for the removal of NO_x pollutants formed in combustion reactions. This work reveals a novel spectral feature for all spectra measured with flowing NO gas present, which we attribute to the interaction of NO with the catalyst. We find that introducing both NO and O_2 gases (compared to only NO) increases the interaction of NO with Cu-SSZ-13. Adsorption of NH_3 leads to a more pronounced spectral signal compared to NO adsorption. For the standard NH_3-SCR reaction, we observe a strong N_2 signal, comprising 30% of the total spectral intensity. These results demonstrate the vast potential of this technique to provide direct, novel insights into the complex interactions between reaction intermediates and the active sites of catalysts, which may guide advanced knowledge-based optimization of these processes.

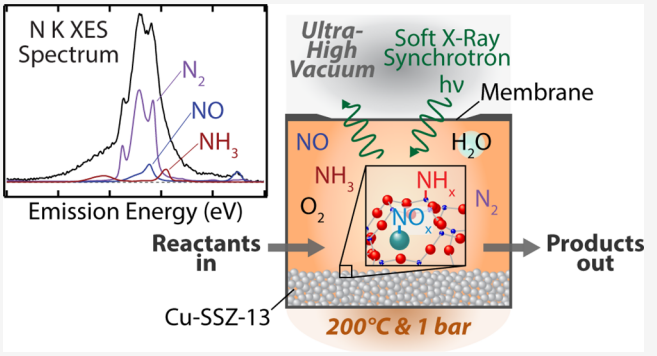

The selective catalytic reduction of nitrogen oxides by ammonia (NH_3-SCR) is a wide-spread process in emission control that is largely used for the conversion of NO_x (primarily NO and NO_2), formed during lean-burn combustion, to more benign molecules, N_2 and H_2O.[1,2] NO_x species cause a wide variety of health and environmental issues; they contribute to the formation of ground-level ozone, smog, and acid rain, but they can also react to form nitrate particles or acid aerosols, all of which can trigger serious respiratory problems. Despite continuing advances in renewable energy technologies and expanding capabilities for CO_2-neutral fuels, it is not unlikely that the global community will continue to rely on internal combustion engines for transportation (e.g., of heavy goods), which currently contribute 14% of global greenhouse gas emissions.[3,4] Moreover, NO_x is formed in many industrial processes and waste incineration plants. Thus, further technology development toward elimination of these emissions is critical.

Zeolite catalysts have been widely applied for use in NH_3-SCR of NO_x. Of particular interest are chabazite-based catalysts, such as Cu-SSZ-13, which have demonstrated excellent performance and stability. While these catalysts have already been commercialized, the exact mechanism including the role of metal centers and zeolite framework is still debated in the literature.[5−12]

Particular focus has recently been laid on understanding the nature and location of Cu species, the special "seagull" activity profile with an activity drop at intermediate temperatures

Received: July 5, 2022
Revised: September 27, 2022
Published: November 30, 2022

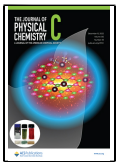

(~350 °C), and the identification of reaction intermediates, mechanisms, and elementary steps. Monomeric/dimeric Cu species[12,13] were reported alongside Cu sites coordinated to a single or two adjacent Al ions of the zeolite framework.[14,15] Additionally, pronounced structural dynamics with altered reactivity were observed as a function of gas mixture and reaction temperature.[6,14,16] With respect to the reaction steps that are necessary to complete the generally accepted $Cu^{2+} \leftrightarrow Cu^{+}$ redox cycle of the SCR mechanism, the adsorption of NH_3 forming $[Cu(NH_3)_x]^+$ complexes is favored as the main intermediate under SCR conditions, especially at low temperatures. *Operando/in situ* characterization of copper sites in Cu-SSZ-13 during SCR of NO_x using hard X-ray emission spectroscopy (XES) and high-energy resolution fluorescence detection X-ray absorption near-edge structure (HERFD-XANES) has confirmed a strong adsorption of NH_3 on Cu, as depicted in Figure 1 (data taken from the

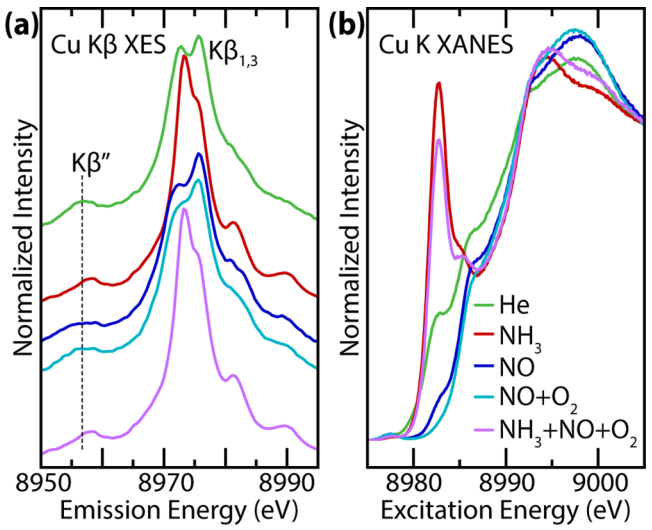

Figure 1. (a) Cu Kβ X-ray emission (XES) and (b) Cu K high-energy resolution X-ray absorption near-edge structure (HERFD-XANES) spectra of 1.2 wt % Cu-SSZ-13 zeolite (Si:Al = 16) measured at 200 °C in He, nitrogen-containing reference gases, and under standard reaction conditions for SCR of NO_x (further details in the experimental series reported in the SI and ref 5).

experimental series in ref 5). A direct interaction between NH_3 and Cu is found, especially evidenced by the shift of the Cu Kβ'' emission line (Figure 1a). Exposure to NO alters the XANES spectrum of Cu sites (Figure 1b), proving the existence of an interaction between Cu and NO in the absence of ammonia and water. This interaction is even more pronounced when a mixture of NO and O_2 is fed over Cu-SSZ-13, particularly at increased temperatures.[6] Upon feeding the standard SCR mixture, the Cu−NH_3 interaction dominates the spectral features below the "seagull" point (~350 °C), leaving interactions with NO undefined; two possibilities are NO adsorption on the same Cu site via O before reacting with NH_3, or NO directly reacting from the gas phase.[6] At higher temperatures, Cu species seem to be more localized at the ion-exchange positions of the zeolite framework due to desorption of water and partially of ammonia, although NO_x adsorption at the Cu sites is facilitated.[6,14,16]

To the best of our knowledge, the results reported in the literature on Cu-SSZ-13 catalysts, including those in Figure 1, provide only indirect information on the actual species adsorbed in the vicinity of Cu sites, which limits the present understanding of the SCR reaction mechanism. Until now, only a limited number of studies have addressed the participation of NH_3 and NO_x stored on the zeolite support.[17] For instance, a multisite mechanism involving ammonia-solvated Cu cations and zeolite Brønsted acid sites (BASs) with formation of H_2NNO and HONO intermediate species was recently suggested by Chen *et al.* and Feng *et al.* based on density functional (DFT) theory calculations and supported by a first-principles microkinetic model.[7,18] The authors also proposed roles for NH_3, depending on its involvement in the reaction mechanism: ligand, inhibiting, and reactant NH_3 at the Cu cations and NH_4^+ at the BAS, in addition to reactant NH_3 gas. Nevertheless, distinguishing between these species or probing rapidly desorbed products such as N_2 or N_2O in the catalyst bed volume is challenging; so far, they have only been detected at the reactor outlet.

To address these open questions, density functional theory (DFT) calculations or experimental infrared (IR) spectroscopy is most often utilized.[5,19−21] However, IR spectroscopy provides only indirect information about chemical bonds that may be related to certain functional groups; this method is insufficient for directly measuring electronic structure information of intermediates. In addition, IR spectroscopy does not account for all N-containing species (e.g., N_2 is not IR-active). Furthermore, the results are difficult to quantify, as molar absorptivity coefficients of various species or functional groups are unknown *a priori*, especially if measurements are made in diffuse reflectance mode (DRIFTS), in which case further factors need to be considered. Finally, overlapping bands from different species in the reaction mixture may severely limit conditions under which IR measurements are possible. Hence, there is a need for a complementary experimental technique, which can directly observe and quantify reacting species, intermediates, and products. Such a technique requires the investigation of light elements with relatively shallow core levels, such as the N and O 1s orbitals of the involved reaction species. Thus, soft X-ray spectroscopy—with its unique capabilities to study the local chemical environment of light elements in solids, liquids, gases, and their interfaces—is a suitable technique to address this challenge.

Among the soft X-ray spectroscopic techniques, X-ray emission spectroscopy (XES) is particularly powerful, as it offers direct insights into the valence electronic structure from the viewpoint of deliberately chosen elements and core levels.[22,23] In our case, it can give a direct view of the occupied valence states responsible for the bond formation between nitrogen-containing molecules and the catalyst surface. Furthermore, as a photon-in-photon-out technique, XES can be combined with custom-designed *in situ* and *operando* cells to also allow for the study of gases, liquids, and their interfaces with solids.[24−31] Such studies have recently become possible due to the major development of high-transmission spectrometers for soft X-rays and of advanced *in situ/operando* cells, as employed in this paper.[29,32,33]

The work presented here uses N K edge XES to investigate interactions between 1.2 wt% Cu-SSZ-13 and various nitrogen-containing gases relevant to SCR of NO_x. To identify the different nitrogen species, we use XES gas phase spectra of NH_3, NO, and N_2, as well *in vacuo* "reference" spectra of NH_3-treated zeolites to analyze *in situ* spectra obtained for zeolites in the presence of NH_3, NO, and O_2 under elevated

https://doi.org/10.1021/acs.jpcc.2c04736
J. Phys. Chem. C 2022, 126, 20998−21009

temperatures. With a detailed fit analysis approach of the spectra taken under reaction conditions, we can identify the presence of nitrogen-containing species at or near the surface of the zeolite.

The XES reference spectra of pure N_2, NH_3, and NO gas are shown in Figure 2a. For the N_2 (g) spectrum, we observe the typical fingerprint reported in previous measurements.[35−39] The spectrum contains three main peaks at 391.5, 393.1, and 394.4 eV, representing electronic transitions with final state holes in the $3\sigma_g$, $1\pi_u$, and $2\sigma_u$ orbitals, respectively. With the high transmission spectrometer used in this study, the underlying vibrational fine structure is not resolved. For the NH_3 (g) spectrum, we observe two dominant peaks, a broad, asymmetric peak at 389.1 eV and a narrow peak at 395.2 eV. Consistent with the previous literature, these are identified as electronic transitions with final state holes in the 1e and $3a_1$ orbitals, respectively.[40−42] Small features are visible in the region between these peaks; these are likely due to double excitations occurring for excitation well above (~20 eV) the absorption edge. For the NO spectrum, we observe an intense, narrow peak at 394.2 eV with a shoulder on the low-energy side, as well as a less intense peak at 402.7 eV. The intense peak and shoulder represent electronic transitions with final state holes in the 5σ and 1π orbitals, respectively.[38] The smaller peak is the N 1s to $2\pi^*$ transition. A more in-depth discussion of NO XES (including the double-excitation peaks indicated with arrows) and resonant inelastic X-ray scattering (RIXS) maps is presented elsewhere.[34]

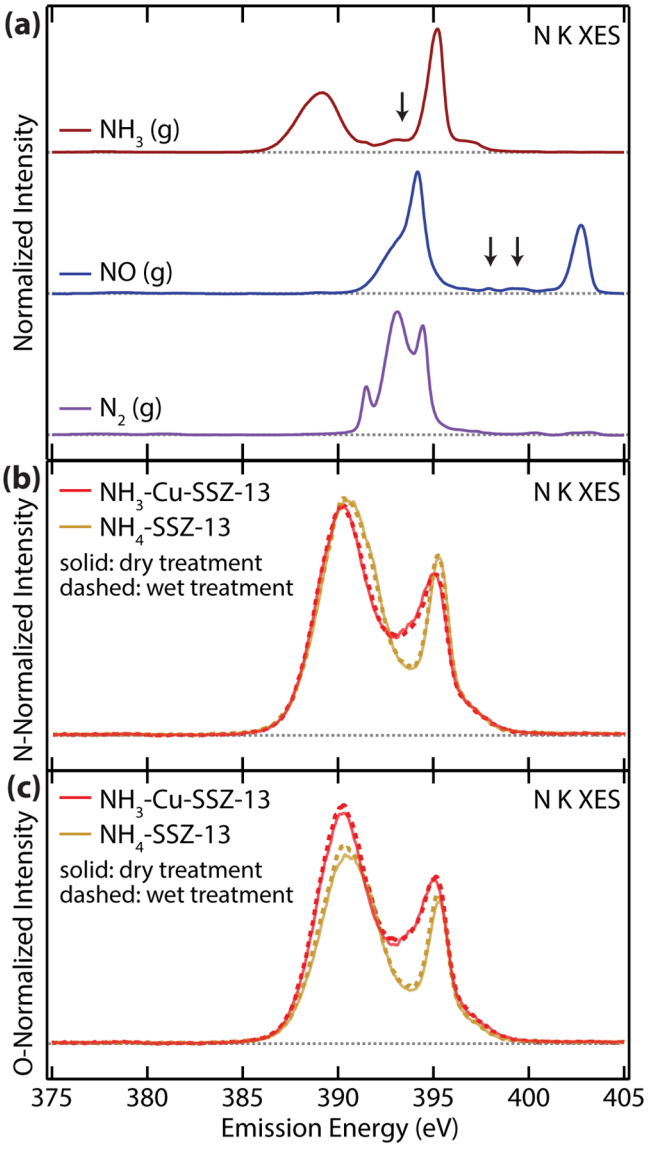

Figure 2. (a) N K X-ray emission (XES) spectra of nitrogen-containing reference gases. Main features are consistent with the established literature results. Arrows indicate small features that are likely due to double excitations.[34] (b, c) N K XES spectra of SSZ-13 zeolites with (red) and without (gold) Cu loading, treated with NH_3 under dry (solid lines) or humidified/wet (dashed lines) conditions. Spectra are normalized to maximum peak height (a), total N XES spectral area (b), and total O XES spectral area (c), the latter to normalize to the overall amount of zeolite present.

To develop a baseline understanding of the interaction between N-containing molecules and the zeolite-based catalysts, we conducted *in vacuo* measurements of both SSZ-13 and Cu-SSZ-13 samples (Si/Al = 16:1, Cu/Al = 1:5) in an ultrahigh vacuum (UHV) environment (base pressure below 10^{-8} mbar). The samples were first pretreated via heating at 500 °C under first 10% O_2 + 1000 ppm NO (1 h) and then 10% O_2 in N_2 (1h) gas flow to remove undesired adsorbates and then treated with NH_3 (g) in either dry (at 100 °C) or 5% water vapor (wet, at 150 °C) conditions (the complete treatment procedure is described in the SI). Figure 2b,c shows the obtained N K XES spectra, with (red) and without (gold) Cu loading. "NH_3-Cu-SSZ-13" is used to designate NH_3-treated Cu-SSZ-13, and "NH_4-SSZ-13" is used to designate NH_3-treated H-SSZ-13. Figure 2b is normalized to the area of the N K XES spectrum to highlight differences in the spectral shape. Figure 2c is normalized to the area of the corresponding O K XES spectra (included in Figure S1 for these and other samples), which approximates a normalization to the total amount of zeolite present in each measurement, as the primary source of the oxygen signal is the aluminosilicate zeolite material. All spectra shown here were measured while scanning across powder samples pressed onto carbon tape at 600 μm/s to minimize beam damage and improve the signal-to-noise ratio. Further details regarding the effect of slower scan rates, the extent of beam damage, and the near-zero N K background signal from the carbon tape are discussed in the SI and illustrated in Figure S1.

Whereas the NH_3 (g) spectrum exhibits two peaks at 389 and 395 eV, the spectra for NH_3-treated zeolites reveal two peaks at 390 and 395 eV (Figure 2), and the valley in-between does not reach near-zero. In a building block picture, the spectra for NH_3-treated zeolites are very similar to those of protonated amino groups,[26,43,44] in accordance with an adsorption as a $-NH_3^+$ species. Here, the narrow feature at 395 eV (present in both cases) is due to ultrafast proton dynamics during the core excitation of the XES measurement, resulting in proton dissociation and formation of $-NH_2$,[26,43,44] while the feature at 390 eV is dominated by contributions of the intact $-NH_4^+$ species.

Comparing the NH_3-treated zeolites, we find a significant difference in shape due to the presence vs absence of Cu (Figure 2b, red vs gold), but there is minimal difference for wet vs dry NH_3 treatment conditions (i.e., dashed vs solid lines). Water is known to compete with NH_3 for binding to Lewis acid sites (LAS) on zeolites; nonetheless, we suspect that the UHV environment removes NH_3 from (weakly bound) LAS in a similar way to that in the presence of water vapors,[6,45]

https://doi.org/10.1021/acs.jpcc.2c04736
J. Phys. Chem. C 2022, 126, 20998−21009

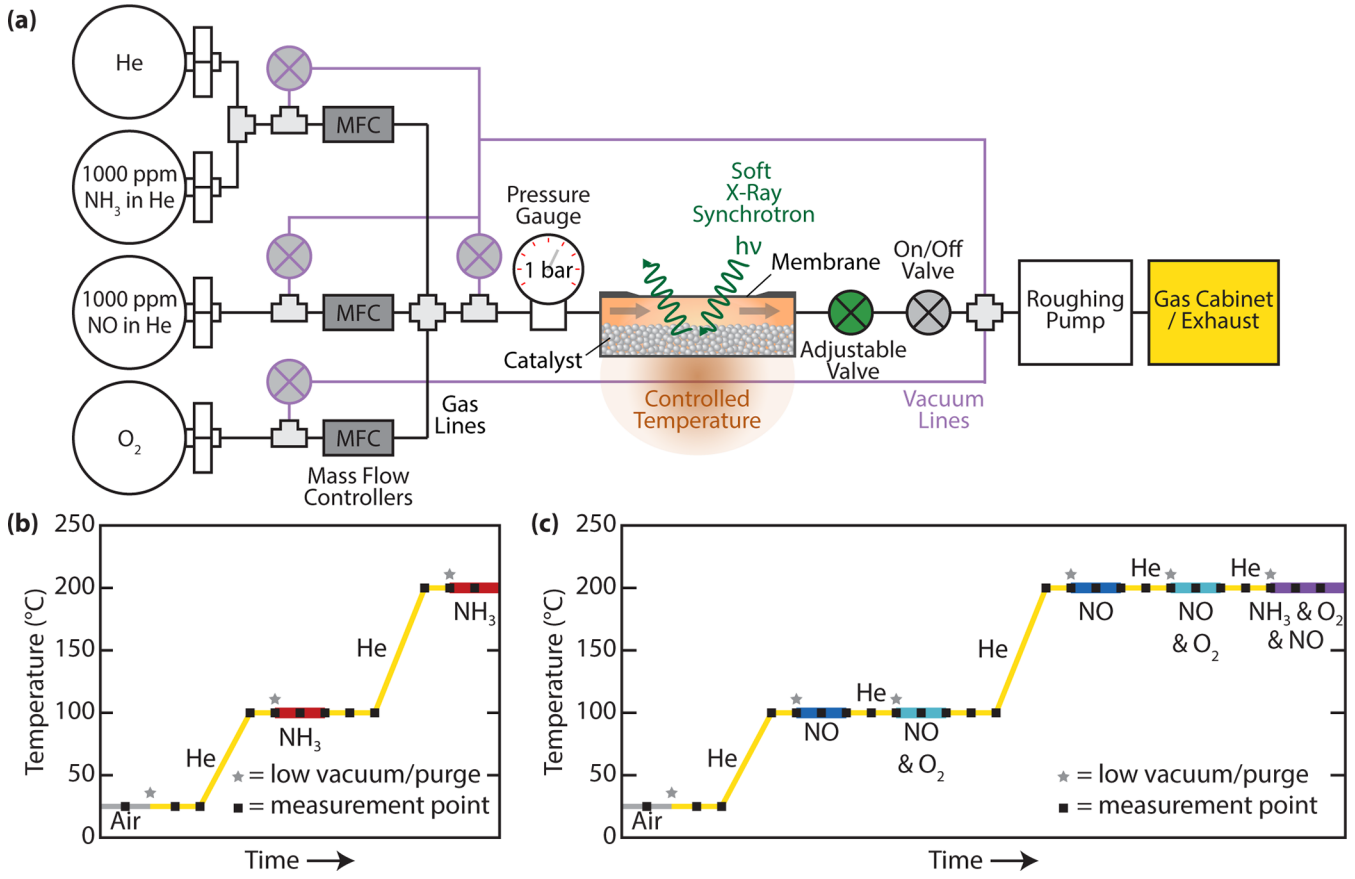

Figure 3. (a) Schematic of the gas manifold and reactor for *in situ* soft XES measurements. (b) One set of experimental conditions and progression of measurements. (c) Second set of experimental conditions and progression of measurements. Both sets were initiated with a fresh catalyst sample, i.e., after pretreatment in dry 1000 ppm NO, 10% O_2 in N_2 balance for 1 h at 500 °C followed by one additional hour at 500 °C in 10% O_2/N_2 to remove adsorbed species. The resulting samples were transported to the ALS in a sealed N_2-purged environment.

resulting in very similar spectra in our *in vacuo* experiments. The gold-colored profiles are, thus, characteristic of NH_4^+ at the BAS. We also observe a significant difference in intensity of the valley region (Figure 2b, ~394 eV) for zeolites with and without Cu. Several effects may be the source of such differences, including the formation of a new molecular orbital or a change in the above-mentioned proton dynamics.

When spectra are normalized to the O K XES area (i.e., proportional to the amount of zeolite present), as in Figure 2c, the area of the N K XES spectra for the Cu-containing powders is approximately 1.3 times larger compared to the Cu-free case. Given this result, we consider that Cu binds NH_3 more strongly than LAS on zeolites, but weaker than BAS on zeolites.[46] BAS are formed near Al atoms, such that the number of BAS is defined by the amount of Al. For Cu-loaded zeolites, Cu^{2+} species can coordinate 3−4 NH_3 groups (~3.3 on average for the used Cu-SSZ-13), depending on their location in the zeolite channels.[21] However, Cu^{2+} species occupy a BAS, thereby increasing NH_3 adsorption by only a factor of ~2.3 per Cu^{2+} site. When reacting with NH_3, a fraction of Cu^{2+} sites reduces to Cu^+, which can coordinate with two NH_3.[21] As this happens, the Cu^+ also detaches from the zeolite framework, leaving a BAS site free to bind another NH_3, enabling a greater increase in the total NH_3 adsorption capacity. Overall, in an ideal case, one may expect an ~40−46% increase in NH_3 adsorption on the used Cu-SSZ-13 zeolite, albeit with considerable room for error due to the remaining uncertainties in NH_3*Cu structures. Therefore, we assign this spectral intensity increase, accompanied by slight variations in peak position, to additional NH_3 adsorbed on the Cu-loaded zeolites. Figure S3 shows the difference between the dry NH_3-Cu-SSZ-13 and dry NH_4-SSZ-13 spectra and illustrates the additional spectral weight, which may represent the interaction between NH_3 and Cu in Cu-SSZ-13. This additional signal, therefore, represents the ligand and inhibiting NH_3 at the Cu cations.

Finally, we note some observable N signal for zeolites that were not subjected to NH_3 treatment, even after the adsorbate-removing pretreatment. These samples exhibited significantly reduced intensity (when normalized to the amount of zeolite), but with similar spectral shapes to those of the NH_3-treated H-SSZ-13 and Cu-SSZ-13 samples. These spectra are included in Figure S2.

Having thus established an *in vacuo* baseline of NH_3-treated zeolite XES spectra (albeit with the caveat that the UHV exposure potentially affected the adsorption of NH_3 on the zeolite materials), we now transition to *in situ* XES experiments to further investigate the interactions between these adsorbates and Cu-SSZ-13. While previously thought impossible due to high absorption and low fluorescence yield of soft X-ray photons in matter, we have developed an *in situ* platform with a custom-designed reactor cell and gas manifold that allows for controlled delivery or purging of gas mixtures, as well as heating of the inlet gases, zeolite, and reaction volume during XES.[29] Combined with a high-flux synchrotron beamline (such as BL8.0.1 at the ALS or the X-SPEC beamline at the KIT-

https://doi.org/10.1021/acs.jpcc.2c04736
J. Phys. Chem. C 2022, 126, 20998−21009

synchrotron[47]) and a high-transmission X-ray spectrometer,[32] it is now possible to conduct such *in situ* (and *operando*) experiments with soft X-ray excitation, enabling us to study the reaction species, i.e., the reactants, intermediates, and products, and not just the catalyst metals.

Most importantly, the reactor design separates the reaction environment (at 25−200 °C and 1 bar) from the UHV environment of the spectrometer and beamline, using a thin SiC membrane (100 nm) that allows soft X-rays to pass with tolerable attenuation (for excitation and emission). The experimental design is illustrated in Figure 3a, and details of the reactor cell are published elsewhere.[29]

Each *in situ* experiment presented here started with a new membrane and a fresh Cu-SSZ-13 catalyst sample, pretreated with NO and O_2 in N_2 and then O_2 in N_2 at 500 °C as described above and transported to the ALS in a sealed N_2-purged environment. Figure 3b,c outlines the experimental conditions, including temperature and gas environment, in the order that they were introduced to the catalyst. In particular, black dots illustrate the sequence and conditions of all measurements (temperature, gas environment, and/or prior low vacuum/purge). The experimental procedure in Figure 3c (NO and O_2 gas conditions followed by the full SCR reaction) was measured before the experimental procedure in Figure 3b (NH_3 gas conditions) to minimize the possibility of residual NH_3 being present during the NO and O_2 gas measurements. These conditions enable analysis of temperature and gas environment effects on adsorption behavior and parallel previous studies on this catalyst.[6] Some of the thus-obtained spectra are shown in Figures 4−6 and will be discussed below.

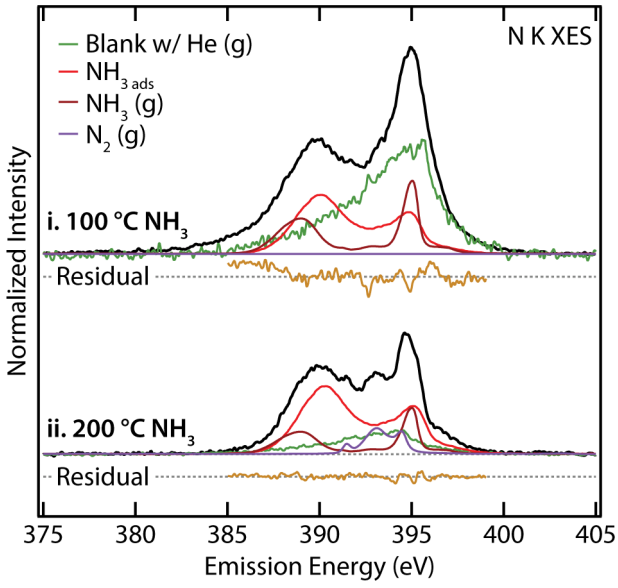

Figure 4. *In situ* N K XES spectra of Cu-SSZ-13 zeolite, exposed to 10 sccm of 1000 ppm NH_3 in He at (i) 100 °C and (ii) 200 °C. Spectra are normalized to measurement time and fit with reference spectra components. The fit residuals are shown below the spectra.

The *in situ* N K XES measurements probe all N-containing species that are present at that particular point of the experimental sequence. In addition to introducing various N-containing species as gaseous reactants, which may adsorb on the catalyst or be present in the gas phase of the reactor, we also observe signal intensity from N-containing species formed

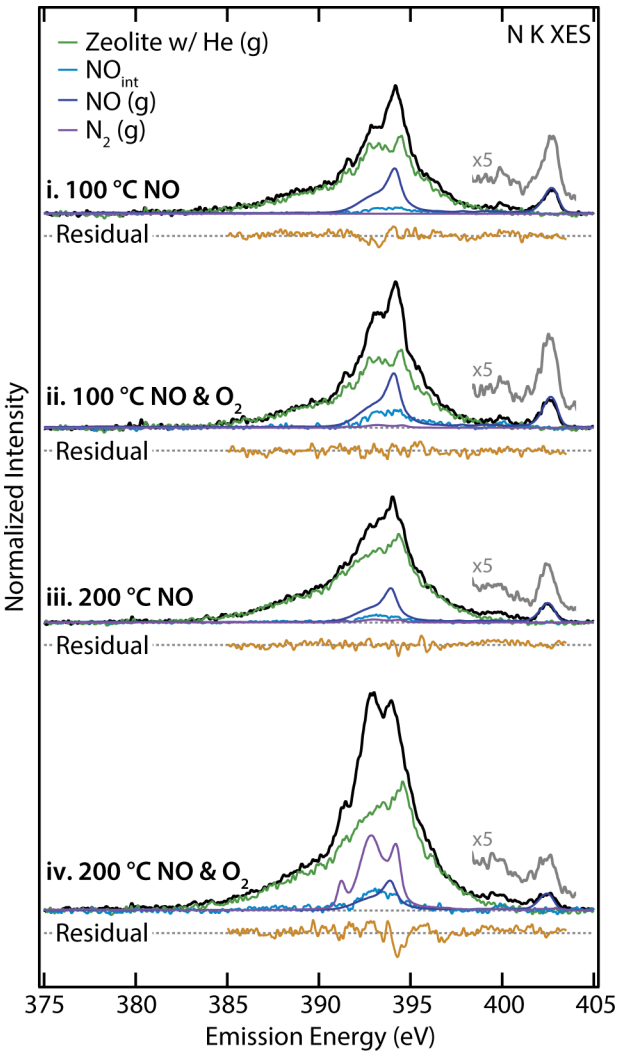

Figure 5. *In situ* N K XES spectra of Cu-SSZ-13 zeolite, exposed to 10 sccm of 1000 ppm NO in He at (i) 100 °C and (iii) 200 °C, and 9 sccm of 1000 ppm NO in He plus 1 sccm O_2 at (ii) 100 °C and (iv) 200 °C. Spectra are normalized to measurement time and fit with reference spectra components. The fit residuals are shown below the spectra.

as intermediates or products. Furthermore, we also need to consider the possibility that N-containing contaminants in our reactor contribute to the spectral signal. Thus, it is also possible that the zeolite or the membrane add some residual background N signal, as observed for the pretreated zeolites in the *in vacuo* measurements. To aid in understanding the data from such complex measurements, Table 1 summarizes the major, medium, and minor contributions to the total N K XES spectrum (top to bottom), and the various experiments in which we expect to detect them (*in vacuo*, *in situ* pure gas references, and *in situ* with zeolites and mixed gases, from right to left). For example, columns E, F, and G refer to the *in situ* reference gas spectra introduced in Figure 2a. Column H refers to the *in vacuo* zeolite measurements introduced in Figure 2b,c. These spectra will be used to identify spectral components of the various species present for the *in situ* zeolite experiments, described in columns A, B, C, and D. The combinations of spectral components that are used to fit the four variants of "Zeolite w/ NX_y (g)" in column A, namely, (1) "Zeolite w/ NH_3", (2) "Zeolite w/ NO", (3) "Zeolite w/ NO & O_2", and

https://doi.org/10.1021/acs.jpcc.2c04736
J. Phys. Chem. C 2022, 126, 20998−21009

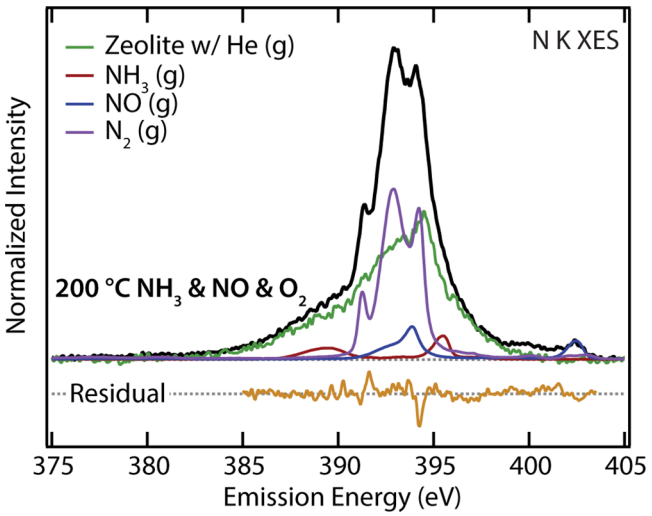

Figure 6. *In situ* N K XES spectrum measured of Cu-SSZ-13 zeolite in a custom reactor cell, under standard reaction conditions for SCR of NO_x with NH_3 (4.5 sccm of 1000 ppm NH_3 in He plus 4.5 sccm of 1000 ppm NO in He plus 1 sccm O_2 at 200 °C). The fit analysis is performed with reference spectra components. The fit residual is shown below the spectra.

(4) "Zeolite w/ NH_3 & NO & O_2", are summarized in Tables S1–S3 (note: variants (2) and (3) are combined in Table S2).

First, *in situ* XES spectra were measured of the empty reactor cell with 10 sccm (standard cubic centimeters per minute) He flowing at room temperature, 100 °C, and 200 °C (Table 1, column D, labeled "Blank w/ He (g)"). This was done to determine the background signal from the membrane and any potential species adsorbed on its surface. Next, spectra were measured for 10 sccm of 1000 ppm NH_3 in He, and for 10 sccm of 1000 ppm NO in He (Table 1, column C, labeled "Blank w/ NO") to determine the relative signal contribution from the dilute gas mixtures, the membrane, and the species adsorbed on the membrane. The final baseline XES measurements were collected for a fresh catalyst in the reactor with He flowing at room temperature, 100 °C, and 200 °C (Table 1, column B, labeled "Zeolite w/ He (g)") to determine a background signal for the zeolite in our experimental setup. This spectrum contains signals from multiple residual nitrogen species that may be adsorbed on the zeolite or on the membrane of the *in situ* cell. Together, these background spectra, combined with the pure gas references and *in vacuo* measurements for NH_3 adsorbed on Cu-SSZ-13, serve to identify various spectral features of N-containing species present during the *in situ* experiments that probe the catalysts with various combinations of dilute NH_3, NO, and O_2 at elevated temperatures.

Following the experimental progression outlined in Figure 3b, a pellet of fresh Cu-SSZ-13 powder catalyst was placed into the reactor cell, put under vacuum ($\sim 10^{-2}$ mbar), and purged several times with He to remove all air. After consistent baseline measurements of zeolite in 1 bar He were obtained, the cell was slowly heated to 100 °C. The pressure in the cell was then reduced to ~1 mbar followed by flowing 10 sccm of 1000 ppm NH_3 in He at 1 bar. Several short XES spectra were recorded for the same condition, inspected for beam damage or other temporal changes, and averaged to improve the signal-to-noise ratio. Each *in situ* spectrum represents steady-state conditions (collected over 25–50 min of total measurement time). In addition, the reactor cell was periodically moved with respect to the beam spot to illuminate a new location on the membrane and minimize beam-induced ad/desorption of species or changes on the membrane. The same procedure was repeated after heating the cell to 200 °C.

The resulting spectra for Cu-SSZ-13 in the presence of flowing dilute NH_3 gas are shown in Figure 4 (black lines). Both spectra were fitted based on the relevant spectral components given in Table 1 and Table S1: empty cell with He flowing (Blank w/ He (g)), representing the background signal for the membrane and any species adsorbed on the membrane (column D), *in vacuo* NH_3-treated Cu-SSZ-13 ($NH_{3\ ads}$), representing the signal from the catalyst and adsorbed NH_3, which includes ligand and inhibiting NH_3 on Cu cations and NH_3 at the BAS (column H), and reference gas

Table 1. Potential N K XES Signal Sources and Relative Magnitude of Signal Contributions (Intensities)

			In situ				Ref			*In vacuo*
		Potential Sources of N K XES Signal	**A** Zeolite w/ NX_y (g)	**B** Zeolite w/ He (g)	**C** Blank w/ NO (g)	**D** Blank w/ He (g)	**E** Ref. NH_3 (g) (High conc.)	**F** Ref. NO (g) (High conc.)	**G** Ref. N_2 (g) (High conc.)	**H** NH_3-treated Zeolite
Signal Contributions	Major	Reactant Gases	**Y**		Y		**Y**	**Y**		
		Product Gases	**Y**						Y	
	Medium	Gases interacting w/ Zeolite	**Y**							Y
		Gases interacting w/ Membrane	**Y**		Y					
	Minor	Zeolite	**Y**	Y						Y
		Membrane	**Y**	Y	Y	Y	*expect relative signal contribution to be very small*			
		Species adsorbed on Membrane	**Y**	Y	Y	Y				

https://doi.org/10.1021/acs.jpcc.2c04736
J. Phys. Chem. C 2022, 126, 20998–21009

spectra for NH_3 and N_2 (columns E and G, respectively). The fit residual (dark orange line) is shown below the measured spectra with a separate dotted gray zero line for reference.

The "Blank w/ He (g)" component has an asymmetric, broad feature at 386−398 eV, with higher intensity toward the high-energy side. Note that the shape of this background spectrum varies slightly with temperature, potentially due to temperature effects on any N content in the membrane or desorption of N species from the reactor walls. The $NH_{3\ ads}$ component, in contrast, has two peaks at 390 and 395 eV (see Figure 2b,c). Likewise, the NH_3 (g) component shows two peaks, but at 389 and 395 eV. The various fit components are thus sufficiently different to allow for a meaningful variation and optimization in the fit routine.

The fits in Figure 4 are normalized to measurement time; because these spectra were measured on the same zeolite pellet, this also normalizes the spectra to the amount of zeolite present. First, we note that the overall spectral intensity is approximately 1.7 times greater at 100 °C vs 200 °C. However, the absolute signal intensity for the $NH_{3\ ads}$ contribution is nearly identical at 100 °C and 200 °C, even though it contributes to a smaller fraction of the total spectral signal at 100 °C (note that a detailed quantitative analysis will be given in conjunction with Figure 7). If no water is present, some

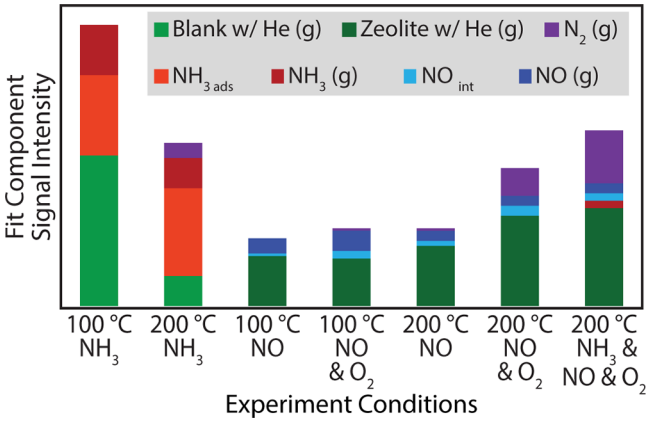

Figure 7. Overview of absolute signal intensities of *in situ* N K edge X-ray emission spectra of Cu-SSZ-13 with their respective fit components for each condition and for each of the species described above. Note that signal intensities are not proportional to the respective concentrations of each species due to variations in absorption cross sections and physical location of each species within the *in situ* reactor cell.

difference is expected in NH_3 adsorption between 100 and 200 °C due to the additional NH_3 adsorption on LAS at lower temperature. However, if water is present (perhaps in small amounts at 100 °C, but not at 200 °C) or if the probing beam is dissociating/removing NH_3 from these sites, little or no difference is anticipated between these two temperatures.[45] Therefore, the spectra suggest that, at 100 °C, some water may still be present and competing with NH_3 for binding sites on the zeolite. At 200 °C, water should be removed, but additional heat/energy input would also remove NH_3 from weakly bound LAS.

The fits also show that the signal intensity for NH_3 (g) is almost double at 100 °C compared to 200 °C. Furthermore, the fits suggests that no N_2 (g) is present at 100 °C, but some N_2 (g) is clearly present at 200 °C, giving rise to the peak at ∼393 eV in the experimental spectrum. Lastly, the fits indicate a vastly different contribution from the background signal at 100 and 200 °C. Time-normalized signal intensities for overall spectra and respective fit components are summarized for all *in situ* measurement conditions in Table S5. As observed in the prior literature, Cu is reduced under NH_3 flow, indicating that Cu sites carry some oxygen, which may possibly oxidize NH_3 to N_2 at 200 °C.[6]

We next discuss the experimental progression outlined in Figure 3c, where a pellet of fresh Cu-SSZ-13 powder catalyst was placed into the reactor cell, exposed to low vacuum (∼1 mbar)/He purge cycles, and then slowly heated before exposure to flowing either 10 sccm of 1000 ppm NO in He, or 9 sccm of 1000 ppm NO in He plus 1 sccm O_2 at 1 bar. The resulting spectra for these two gas conditions, measured both at 100 and 200 °C, are shown in Figure 5. Similar to the NH_3 gas conditions, these spectra were fit with appropriate spectral components to identify signal contributions according to Table 1 and Table S2. In this case, we do not have an *ex situ* or *in vacuo* NO-treated Cu-SSZ-13 spectrum to represent adsorbed NO, since only very small amounts of NO are expected to adsorb.[46] Günter *et al.* showed that, at temperatures below 200 °C, the presence of small traces of H_2O (readsorbed on the catalyst surface during sample manipulation) was found to inhibit the interaction of NO with Cu sites in Cu-SSZ-13 catalyst.[5,46] In other works, harsh *in situ* pretreatments in dry conditions, such as annealing at 500 °C under high vacuum, calcination at 400 °C, or reduction at 550 °C, were required to detect any interaction of Cu-SSZ-13 with NO.[5,48,49] Hence, in this study, we used a combination of other measured spectra to estimate a spectral shape for NO that is adsorbed or otherwise interacting with an available surface (catalyst site or membrane, labeled "NO_{int}").

This "NO_{int}" component (column "C−D−F" in Table S2) was calculated separately for 100 and 200 °C and in both cases included a dominant feature at 392−395 eV as well as a unique feature at approximately 400 eV. Some contribution of this feature at 400 eV was observed in all spectra measured with flowing NO gas present and may be the main indicator of NO interaction with other species. Note that the spectral shape was estimated from differences of other spectra and that the true spectral shape for adsorbed NO (or interacting with other species) likely also contains similar peaks as measured for NO (g). For purposes of fitting, 100% of the NO-related peak intensity at 402.5 eV was subtracted to isolate the unique peak at 400 eV in this fit component. Unlike the $NH_{3\ ads}$ spectrum, the NO_{int} spectra do not include a signal contribution from the zeolite; therefore, the "Zeolite w/ He (g)" spectrum was used to represent the background signal for these conditions. The "Zeolite w/ He (g)" spectrum consists of a broad main feature at 390−397 eV and has slightly different shapes at 100 and 200 °C, potentially due to temperature effects on the N content in the zeolite. The overall spectra are again normalized to time as an approximate normalization to zeolite content; they display nearly similar intensity for all NO conditions shown in Figure 5, except for the 200 °C NO & O_2 condition, for which the overall spectral intensity doubles.

The fits for the first three conditions (NO at 100 °C and 200 °C, NO & O_2 at 100 °C) reflect a similar relative contribution of the background Zeolite w/ He (g) signal, while a slightly greater contribution is found for the 200 °C NO & O_2 condition. Fits also suggest no (or very little) signal intensity from N_2 (g), while, again, the 200 °C NO and O_2 condition

https://doi.org/10.1021/acs.jpcc.2c04736
J. Phys. Chem. C 2022, 126, 20998−21009

features a clear N_2 (g) contribution, comprising ~19% of the spectral area. Decomposition of NO to N_2 and O_2 occurs on Cu zeolites, but the presence of O_2 should inhibit this process.[50] Therefore, we would not necessarily expect to observe more N_2 in the presence of O_2. We speculate that this may be due to trace NH_3 in the zeolite, as observed in the untreated *in vacuo* samples (Figure S1, top right). NH_3 likely reacts with NO to form small amounts of N_2. Additionally, we note that this N_2 signal stems from the spectroscopic probe volume, which includes the volume of gas above the zeolite, gas in the pores of the zeolite, adsorbates on the zeolite, and the zeolite itself, while we have not analyzed the product stream leaving the cell (as is most often characterized in the prior literature).

The fits in Figure 5 reflect similar levels of signal intensity from NO (g) at 100 °C, and lower, but similar, signal intensity at the two 200 °C conditions. Lastly, the fits suggest low levels of signal intensity from the calculated NO_{int} component for NO-only conditions, but an increased intensity (~3×) for both NO & O_2 conditions. Compared to the NH_3 conditions in Figure 4, the NO conditions lead to a lower N K signal intensity (i.e., for adsorbed NO vs NH_3 species), although the presence of O_2 may aid in NO adsorption. This observation is consistent with temperature-programmed desorption results (not shown) and complementary to our hard X-ray studies (Figure 1), which for such low temperatures indicate less interaction between Cu zeolites and NO compared to NH_3 and increased interaction between Cu and NO in the presence of O_2.[6,46] These studies also showed that, compared to NO, the presumably formed NO_2 and NO_3^- do indeed show a prominent interaction with Cu sites in Cu-SSZ-13. However, under the experimental conditions in our current investigation, the formation of nitrate and nitrite species via NO oxidation was not identified; a detailed analysis is given in the SI (Figure S4). Instead, it was observed that the introduction of NO and O_2 to the catalyst lead to an increase of the amount of NO interacting with the zeolite (NO_{int} component), which also contributes to the spectral feature at ~400 eV. Indeed, soft XES investigations of NO adsorption on well-defined ruthenium surfaces have identified a reorganization of electron distribution and the formation of new hybridized chemisorbate orbitals.[51] Simulated XES spectra also show peaks in this energy range that are associated with molecular orbitals formed via chemisorption of NO.[52] These features are distinct and more intense than other possible satellite features (resulting from free NO (g)) in this energy region.[34,53] Therefore, we highlight NO_{int} as an important fit component, with a unique identifying spectral feature at ~400 eV that we attribute to interactions of NO with Cu-SSZ-13. An extended analysis of these features is included in Section 7 of the SI.

As the culminating experimental step, the Cu-SSZ-13 catalyst was exposed to reaction conditions for standard SCR, using 4.5 sccm of 1000 ppm NH_3 in He, plus 4.5 sccm of 1000 ppm NO in He, and plus 1 sccm O_2, at 200 °C. The resulting spectrum is shown in Figure 6, together with the same fit components as used for the previous NO-containing conditions. Many iterations of fits were performed before identifying this as the best representation; a comparison of possible satisfactory fits is shown in Figure S5. The small variations in the fits indicate that the fit results are quite robust, regardless of choice of background signal ("Zeolite w/ He (g)" or "Blank w/ He (g)").

None of the attempted fits suggested a significant spectral intensity contribution from the *in vacuo* spectrum representing $NH_{3\ ads}$, and thus this component has been removed from the figures for clarity. However, this does not exclude that NH_3 may still be adsorbed in small amounts on the zeolite, represented in the "Zeolite w/ He (g)" background signal. Potential beam-induced desorption of NH_3 may have reduced the intensity of this spectral contribution, as illustrated in Figure S1. Additionally, an increased presence of N-containing gas phase species under these conditions may also mask a (small) signal from adsorbed NH_3, since the exciting and emitted photons need to travel through the gas phase to/from the zeolite at the back of the *in situ* reactor cell. Lastly, it is possible that NH_3 is adsorbed in a different manner for this *in situ* reaction (e.g., "reactant NH_3", which could not be observed under reference conditions) than that measured for the *in vacuo* samples, and thus the spectral signal for this species may be slightly different.

In contrast, all fits of the experimental spectrum in Figure 6 show a very strong contribution of N_2 (g) (~30% of the total signal), in agreement with the clearly observed presence of a peak at ~391.5 eV in the experimental spectrum. Since N_2 (g) was not fed over the catalyst, we identify this species as an SCR reaction-facilitated product. In addition, small contributions are observed for NH_3 (g) and NO (g) (~4% and ~6%, respectively). When included in two of the fits in Figure S5b,d, the NO_{int} component represents approximately 5% of the total spectral area; inclusion of this peak is compensated for by a slight decrease in the "Zeolite w/ He (g)" or "Blank w/ He (g)" background and N_2 (g) signals.

When normalized to measurement time (and amount of zeolite), the overall spectral area for the standard reaction condition is ~1.3 times greater than for the 200 °C NO & O_2 condition. Therefore, the absolute signal intensity from N_2 (g) is ~1.9 times greater for the complete reaction mixture, compared to the 200 °C NO & O_2 condition. While this N_2 signal may be lower than expected for the product stream of Cu-SSZ-13 under these conditions, it is again important to note that this technique probes all species present in the reaction cell (and not in the product stream). It is likely that gas in the volume above the zeolite is removed from the cell more quickly under constant flow conditions than gas species that diffuse into the zeolite pores. Depending on the adsorption constants of the various gas species, it is possible that some gas species have a longer residence time in the pores of the zeolite and thus remain in the reactor cell and show greater contributions to the overall spectrum. Finally, the NO conversion is expected to be relatively low at this temperature.[5]

Figure 7 shows a summary of the relative intensities of the respective spectral fit components for each of the experimental conditions presented in this paper (also quantified in Table S4). The total height of each bar is proportional to the overall spectral intensity for each condition, while colored segments represent the area of each fit component. This representation does not indicate absolute concentration of the species present in the reactor cell, as the relative absorption cross sections of each species as well as their concentration gradient within the cell differ and cannot be accurately quantified. In addition, further species may form that are possibly contained in the "Zeolite w/ He (g)" background. This summary plot shows the approximately equal $NH_{3\ ads}$ signal intensity for the two NH_3 conditions and reflects the slightly increased NO_{int} intensity for the NO & O_2 conditions vs the NO-only conditions. Most

https://doi.org/10.1021/acs.jpcc.2c04736
J. Phys. Chem. C 2022, 126, 20998−21009

noteworthily, contributions of N_2 (g) are also shown (purple, top-most species for the 200 °C conditions).

In conclusion, we have probed the electronic structure of reaction species, including reactants, intermediates, spectator species, and products, involved in the standard SCR reaction over Cu-SSZ-13 using soft XES and our custom-designed *in situ* reactor cell. N K XES provides a direct view of the occupied valence states responsible for the bond formation between nitrogen-containing molecules and the catalyst surface, enabling us to distinguish free vs adsorbed species. For this analysis, we first established a set of references, measuring N K XES spectra of pure NH_3, NO, and N_2 gas, which would later become the reactants and products of the *in situ* measurements of the complete SCR reaction. *In vacuo* measurements of NH_3-treated SSZ-13 zeolites with and without Cu also revealed differences in spectral shape and intensity, which we attribute to additional NH_3 adsorption on the Cu-loaded zeolites. Further investigation of the NH_3 interaction with Cu-SSZ-13 catalysts using *in situ* measurements at 100 and 200 °C showed a similar intensity for the $NH_{3\ ads}$ fit component, suggesting that a competition between NH_3 and H_2O at 100 °C and desorption due to increased thermal energy at 200 °C results in similar levels of NH_3 adsorption at these temperatures.

Next, we have investigated the interaction between NO and Cu-SSZ-13 and examined the effects of temperature as well as the presence/absence of O_2. We have identified a unique spectral feature at ∼400 eV that was observed in all spectra measured with flowing NO gas present. This feature does not align with identified peaks or satellite features for free NO (g), nitrite, or nitrate reference species and thus may be a unique indicator of NO interaction with other surface sites. The intensity of this feature is increased by ∼3× for conditions that include both NO and O_2 gas, compared to only NO gas. Therefore, we attribute this peak to represent interactions of NO with the zeolite matrix, Cu, or other species and find that introducing NO and O_2 gases increases the interaction of NO with the Cu-SSZ-13. Computational investigations will likely be required to further unravel the origin of this feature.

Finally, N K XES was measured for Cu-SSZ-13 exposed to the standard reaction conditions for SCR of NO_x with NH_3. Multiple fits were used to assess the choice of fit components and background signal; the presence of only small variations in the fits indicate that the results are quite robust. The fits reveal the strongest signal contribution for N_2 (∼30% of total intensity) compared to any other conditions. We also note some signal contribution from free NH_3 and NO gas as well as, possibly, from NO interactions with the zeolite (when this component was included). Supporting the conclusion derived from the earlier and complementary hard X-ray study,[6] an interaction of NO with the Cu and BAS of the zeolite was shown to be weak, amounting to less than 5% of N atoms in the reaction system. In addition, our analysis emphasizes the advantage of probing the Cu-N interaction from the viewpoint of both the N K-edge and the Cu K-edge.

This work thus brings together advances in high-flux synchrotron beamlines, a high-transmission X-ray spectrometer, and an *in situ* platform with a custom-designed reactor cell and gas manifold to enable *in situ* (and *operando*) experiments with soft X-ray excitation. Our spectral analysis applies a consistent fitting scheme to all *in situ* experimental conditions, allowing robust comparisons of species across a range of controlled catalyst environments, including varied gas composition and temperatures, to reveal trends and identify unique spectral features which represent interaction between reaction intermediates and catalyst surfaces. We highlight the use of *in situ* (and *operando*) experiments with soft X-ray excitation to study the local chemical environment of light elements, which provides powerful and complementary insights to hard X-ray investigations of catalyst materials. As is the case with hard X-ray spectroscopy, the combination of XES (probing occupied electronic levels) and XANES (probing unoccupied electronic levels) allows for a comprehensive description of electronic structure of reactants, intermediates, and products.[54]

■ ASSOCIATED CONTENT

Supporting Information

The Supporting Information is available free of charge at https://pubs.acs.org/doi/10.1021/acs.jpcc.2c04736.

Sample preparation, experimental methods, mitigating effects of beam damage, comparison of normalization schemes for *in vacuo* XES spectra of Cu-SSZ-13, fitting components for *in situ* N K XES measurement conditions, summary of signal intensities for *in situ* N K XES of Cu-SSZ-13 zeolite, comparison of features for NO_x reference and *in situ* spectra, additional fits for *in situ* XES spectra of the full SCR reaction, references (PDF)

■ AUTHOR INFORMATION

Corresponding Authors

Linsey C. Seitz − *Institute for Photon Science and Synchrotron Radiation (IPS), Karlsruhe Institute of Technology (KIT), 76344 Eggenstein-Leopoldshafen, Germany; Department of Chemical and Biological Engineering, Northwestern University, Evanston, Illinois 60208, United States;* orcid.org/0000-0001-6831-6747; Email: linsey.seitz@northwestern.edu

Lothar Weinhardt − *Institute for Photon Science and Synchrotron Radiation (IPS), Karlsruhe Institute of Technology (KIT), 76344 Eggenstein-Leopoldshafen, Germany; Institute for Chemical Technology and Polymer Chemistry (ITCP), Karlsruhe Institute of Technology (KIT), 76131 Karlsruhe, Germany; Department of Chemistry and Biochemistry, University of Nevada Las Vegas (UNLV), Las Vegas, Nevada 89154-4003, United States;* orcid.org/0000-0003-3361-1054; Email: lothar.weinhardt@kit.edu

Authors

Dmitry E. Doronkin − *Institute for Chemical Technology and Polymer Chemistry (ITCP), Karlsruhe Institute of Technology (KIT), 76131 Karlsruhe, Germany; Institute of Catalysis Research and Technology (IKFT), Karlsruhe Institute of Technology (KIT), 76344 Eggenstein-Leopoldshafen, Germany;* orcid.org/0000-0003-3930-3204

Dirk Hauschild − *Institute for Photon Science and Synchrotron Radiation (IPS), Karlsruhe Institute of Technology (KIT), 76344 Eggenstein-Leopoldshafen, Germany; Institute for Chemical Technology and Polymer Chemistry (ITCP), Karlsruhe Institute of Technology (KIT), 76131 Karlsruhe, Germany; Department of Chemistry and Biochemistry, University of Nevada Las Vegas (UNLV), Las*

https://doi.org/10.1021/acs.jpcc.2c04736
J. Phys. Chem. C 2022, 126, 20998−21009

Vegas, Nevada 89154-4003, United States; orcid.org/0000-0001-9088-8944

Maria Casapu − *Institute for Chemical Technology and Polymer Chemistry (ITCP), Karlsruhe Institute of Technology (KIT), 76131 Karlsruhe, Germany;* orcid.org/0000-0002-8755-9856

Deniz Zengel − *Institute for Chemical Technology and Polymer Chemistry (ITCP), Karlsruhe Institute of Technology (KIT), 76131 Karlsruhe, Germany*

Anna Zimina − *Institute for Chemical Technology and Polymer Chemistry (ITCP), Karlsruhe Institute of Technology (KIT), 76131 Karlsruhe, Germany; Institute of Catalysis Research and Technology (IKFT), Karlsruhe Institute of Technology (KIT), 76344 Eggenstein-Leopoldshafen, Germany;* orcid.org/0000-0002-3111-7741

Dagmar Kreikemeyer-Lorenzo − *Institute for Photon Science and Synchrotron Radiation (IPS), Karlsruhe Institute of Technology (KIT), 76344 Eggenstein-Leopoldshafen, Germany*

Monika Blum − *Advanced Light Source (ALS), Lawrence Berkeley National Laboratory, Berkeley, California 94720, United States; Chemical Sciences Division, Lawrence Berkeley National Laboratory, Berkeley, California 94720, United States;* orcid.org/0000-0002-2918-9092

Wanli Yang − *Advanced Light Source (ALS), Lawrence Berkeley National Laboratory, Berkeley, California 94720, United States;* orcid.org/0000-0003-0666-8063

Jan-Dierk Grunwaldt − *Institute for Chemical Technology and Polymer Chemistry (ITCP), Karlsruhe Institute of Technology (KIT), 76131 Karlsruhe, Germany; Institute of Catalysis Research and Technology (IKFT), Karlsruhe Institute of Technology (KIT), 76344 Eggenstein-Leopoldshafen, Germany;* orcid.org/0000-0003-3606-0956

Clemens Heske − *Institute for Photon Science and Synchrotron Radiation (IPS), Karlsruhe Institute of Technology (KIT), 76344 Eggenstein-Leopoldshafen, Germany; Institute for Chemical Technology and Polymer Chemistry (ITCP), Karlsruhe Institute of Technology (KIT), 76131 Karlsruhe, Germany; Department of Chemistry and Biochemistry, University of Nevada Las Vegas (UNLV), Las Vegas, Nevada 89154-4003, United States;* orcid.org/0000-0001-7586-4549

Complete contact information is available at: https://pubs.acs.org/10.1021/acs.jpcc.2c04736

Author Contributions

LCS planned and performed spectroscopy measurements. Completed all data analysis. Wrote first draft and managed / contributed to editing process for main text and SI. DED, DZ, and MC contributed to the synthesis, characterization, and pre-treatment of Cu-SSZ-13, as well as to the *in situ* Cu Kβ XES and HERFD XANES measurements; they also helped in drafting the paper. DH, DKL, MB, LW, and WY supported spectroscopy measurements. LW, JDG, MC, and CH designed the study and helped in drafting the paper. All authors have contributed to the scientific discussion, the manuscript editing process, and have given approval to the final version of the manuscript.

Funding

This work was supported by the Helmholtz Association via Grant No. PD-326.

Notes

The authors declare no competing financial interest.

■ ACKNOWLEDGMENTS

This research used resources of the Advanced Light Source, which is a DOE Office of Science User Facility under contract no. DE-AC02-05CH11231. The authors thank Tobias Günter for the synthesis of parent SSZ-13 zeolite. The authors also thank Doug Taube at the Lawrence Berkeley National Lab, without whom these experiments would not have been possible. L.S. acknowledges support from the Helmholtz Association via Grant PD-326. J.D.G. thanks for support through DFG (GR 3987/5-1) and beamtime at ID 26 at ESRF for hard XES and HERFD-XANES measurements.

■ ABBREVIATIONS

BAS, Brønsted acid sites; DFT, density functional theory; DRIFTS, diffuse reflectance infrared Fourier transform spectroscopy; HERFD, high energy resolution fluorescence detection; IR, infrared spectroscopy; LAS, Lewis acid sites; NH_3-SCR of NO_x, selective catalytic reduction of nitrogen oxides with ammonia; RIXS, resonant inelastic X-ray scattering; UHV, ultrahigh vacuum; XANES, X-ray absorption near edge structure; XES, X-ray emission spectroscopy

■ REFERENCES

(1) Alkemade, U. G.; Schumann, B. Engines and exhaust after treatment systems for future automotive applications. *Solid State Ionics* **2006**, *177*, 2291−2296.

(2) Nova, I.; Tronconi, E. *Urea-SCR Technology for deNO$_x$ After Treatment of Diesel Exhausts*. Springer New York: 2014

(3) Lambert, C. K. Current state of the art and future needs for automotive exhaust catalysis. *Nat. Catal.* **2019**, *2*, 554−557.

(4) Edenhofer, O.; Sokona, Y.; Farahani, E.; Kadner, S.; Seyboth, K.; Adler, A.; Baum, I.; Brunner, S.; Eickemeier, P.; Kriemann, B.; Savolainen, J.; Schlömer, S.; von Stechow, C.; Zwickel, T.; Minx, J. C. (eds.) *IPCC, 2014: Climate Change 2014: Mitigation of Climate Change. Contribution of Working Group III to the Fifth Assessment Report of the Intergovernmental Panel on Climate Change*; Cambridge University Press: Cambridge, United Kingdom and New York, NY, USA, 2014.

(5) Günter, T.; Carvalho, H. W. P.; Doronkin, D. E.; Sheppard, T.; Glatzel, P.; Atkins, A. J.; Rudolph, J.; Jacob, C. R.; Casapu, M.; Grunwaldt, J.-D. Structural snapshots of the SCR reaction mechanism on Cu-SSZ-13. *Chem. Commun.* **2015**, *51*, 9227−9230.

(6) Fahami, A. R.; Günter, T.; Doronkin, D. E.; Casapu, M.; Zengel, D.; Vuong, T. H.; Simon, M.; Breher, F.; Kucherov, A. V.; Brückner, A.; Grunwaldt, J. D. The dynamic nature of Cu sites in Cu-SSZ-13 and the origin of the seagull NO_x conversion profile during NH_3-SCR. *React. Chem. Eng.* **2019**, *4*, 1000−1018.

(7) Chen, L.; Janssens, T. V. W.; Vennestrøm, P. N. R.; Jansson, J.; Skoglundh, M.; Grönbeck, H. A Complete Multisite Reaction Mechanism for Low-Temperature NH_3-SCR over Cu-CHA. *ACS Catal.* **2020**, *10*, 5646−5656.

(8) Janssens, T. V. W.; Falsig, H.; Lundegaard, L. F.; Vennestrøm, P. N. R.; Rasmussen, S. B.; Moses, P. G.; Giordanino, F.; Borfecchia, E.; Lomachenko, K. A.; Lamberti, C.; Bordiga, S.; Godiksen, A.; Mossin, S.; Beato, P. A Consistent Reaction Scheme for the Selective Catalytic Reduction of Nitrogen Oxides with Ammonia. *ACS Catal.* **2015**, *5*, 2832−2845.

(9) Marberger, A.; Petrov, A. W.; Steiger, P.; Elsener, M.; Kröcher, O.; Nachtegaal, M.; Ferri, D. Time-resolved copper speciation during

selective catalytic reduction of NO on Cu-SSZ-13. *Nat. Catal.* **2018**, *1*, 221−227.
(10) Paolucci, C.; Di Iorio, J. R.; Ribeiro, F. H.; Gounder, R.; Schneider, W. F., Chapter One - Catalysis Science of NO_x Selective Catalytic Reduction With Ammonia Over Cu-SSZ-13 and Cu-SAPO-34. In *Advances in Catalysis*, Song, C., Ed. Academic Press: 2016; Vol. *59*, pp. 1−107.
(11) Paolucci, C.; Parekh, A. A.; Khurana, I.; Di Iorio, J. R.; Li, H.; Albarracin Caballero, J. D.; Shih, A. J.; Anggara, T.; Delgass, W. N.; Miller, J. T.; Ribeiro, F. H.; Gounder, R.; Schneider, W. F. Catalysis in a Cage: Condition-Dependent Speciation and Dynamics of Exchanged Cu Cations in SSZ-13 Zeolites. *JACS* **2016**, *138*, 6028−6048.
(12) Paolucci, C.; Khurana, I.; Parekh, A. A.; Li, S.; Shih, A. J.; Li, H.; Di Iorio, J. R.; Albarracin-Caballero, J. D.; Yezerets, A.; Miller, J. T.; Delgass, W. N.; Ribeiro, F. H.; Schneider, W. F.; Gounder, R. Dynamic multinuclear sites formed by mobilized copper ions in NO_x selective catalytic reduction. *Science* **2017**, *357*, 898.
(13) Psofogiannakis, G. M.; McCleerey, J. F.; Jaramillo, E.; van Duin, A. C. T. ReaxFF Reactive Molecular Dynamics Simulation of the Hydration of Cu-SSZ-13 Zeolite and the Formation of Cu Dimers. *JPCC* **2015**, *119*, 6678−6686.
(14) Bates, S. A.; Verma, A. A.; Paolucci, C.; Parekh, A. A.; Anggara, T.; Yezerets, A.; Schneider, W. F.; Miller, J. T.; Delgass, W. N.; Ribeiro, F. H. Identification of the active Cu site in standard selective catalytic reduction with ammonia on Cu-SSZ-13. *J Cat* **2014**, *312*, 87−97.
(15) Deka, U.; Lezcano-Gonzalez, I.; Warrender, S. J.; Lorena Picone, A.; Wright, P. A.; Weckhuysen, B. M.; Beale, A. M. Changing active sites in Cu−CHA catalysts: deNO$_x$ selectivity as a function of the preparation method. *Microporous Mesoporous Mater.* **2013**, *166*, 144−152.
(16) Gao, F.; Peden, C. H. F. Recent Progress in Atomic-Level Understanding of Cu/SSZ-13 Selective Catalytic Reduction Catalysts. *Catalysts* **2018**, *8*, 140.
(17) Zhu, H.; Kwak, J. H.; Peden, C. H. F.; Szanyi, J. In situ DRIFTS-MS studies on the oxidation of adsorbed NH_3 by NO_x over a Cu-SSZ-13 zeolite. *Catal. Today* **2013**, *205*, 16−23.
(18) Feng, Y.; Wang, X.; Janssens, T. V. W.; Vennestrøm, P. N. R.; Jansson, J.; Skoglundh, M.; Grönbeck, H. First-Principles Microkinetic Model for Low-Temperature NH_3-Assisted Selective Catalytic Reduction of NO over Cu-CHA. *ACS Catal.* **2021**, *11*, 14395−14407.
(19) Paolucci, C.; Verma, A. A.; Bates, S. A.; Kispersky, V. F.; Miller, J. T.; Gounder, R.; Delgass, W. N.; Ribeiro, F. H.; Schneider, W. F. Isolation of the Copper Redox Steps in the Standard Selective Catalytic Reduction on Cu-SSZ-13. *Angew. Chem., Int. Ed.* **2014**, *53*, 11828−11833.
(20) Borfecchia, E.; Lomachenko, K. A.; Giordanino, F.; Falsig, H.; Beato, P.; Soldatov, A. V.; Bordiga, S.; Lamberti, C. Revisiting the nature of Cu sites in the activated Cu-SSZ-13 catalyst for SCR reaction. *Chem Science* **2015**, *6*, 548−563.
(21) Kerkeni, B.; Berthout, D.; Berthomieu, D.; Doronkin, D. E.; Casapu, M.; Grunwaldt, J. D.; Chizallet, C. Copper Coordination to Water and Ammonia in Cu^{II}-Exchanged SSZ-13: Atomistic Insights from DFT Calculations and in Situ XAS Experiments. *JPCC* **2018**, *122*, 16741−16755.
(22) Nilsson, A.; Hasselström, J.; Föhlisch, A.; Karis, O.; Pettersson, L. G. M.; Nyberg, M.; Triguero, L. Probing chemical bonding in adsorbates using X-ray emission spectroscopy. *J. Electron Spectrosc. Relat. Phenom.* **2000**, *110-111*, 15−39.
(23) Nilsson, A.; Pettersson, L. G. M. Chemical bonding on surfaces probed by X-ray emission spectroscopy and density functional theory. *Surf. Sci. Rep.* **2004**, *55*, 49−167.
(24) Fuchs, O.; Maier, F.; Weinhardt, L.; Weigand, M.; Blum, M.; Zharnikov, M.; Denlinger, J.; Grunze, M.; Heske, C.; Umbach, E. A liquid flow cell to study the electronic structure of liquids with soft X-rays. *Nucl. Instrum. Methods Phys. Res., Sect. A* **2008**, *585*, 172−177.
(25) Blum, M.; Weinhardt, L.; Fuchs, O.; Bär, M.; Zhang, Y.; Weigand, M.; Krause, S.; Pookpanratana, S.; Hofmann, T.; Yang, W.; Denlinger, J. D.; Umbach, E.; Heske, C. Solid and liquid spectroscopic analysis (SALSA)−a soft x-ray spectroscopy endstation with a novel flow-through liquid cell. *Rev. Sci. Instrum.* **2009**, *80*, 123102.
(26) Blum, M.; Odelius, M.; Weinhardt, L.; Pookpanratana, S.; Bär, M.; Zhang, Y.; Fuchs, O.; Yang, W.; Umbach, E.; Heske, C. Ultrafast Proton Dynamics in Aqueous Amino Acid Solutions Studied by Resonant Inelastic Soft X-ray Scattering. *JPCB* **2012**, *116*, 13757−13764.
(27) Weinhardt, L.; Benkert, A.; Meyer, F.; Blum, M.; Wilks, R. G.; Yang, W.; Bär, M.; Reinert, F.; Heske, C. Nuclear dynamics and spectator effects in resonant inelastic soft x-ray scattering of gas-phase water molecules. *J. Chem. Phys.* **2012**, *136*, 144311.
(28) Weinhardt, L.; Blum, M.; Fuchs, O.; Benkert, A.; Meyer, F.; Bär, M.; Denlinger, J. D.; Yang, W.; Reinert, F.; Heske, C. RIXS investigations of liquids, solutions, and liquid/solid interfaces. *J. Electron Spectrosc. Relat. Phenom.* **2013**, *188*, 111−120.
(29) Benkert, A.; Blum, M.; Meyer, F.; Wilks, R. G.; Yang, W.; Bär, M.; Reinert, F.; Heske, C.; Weinhardt, L. Setup for in situ investigation of gases and gas/solid interfaces by soft x-ray emission and absorption spectroscopy. *Rev. Sci. Instrum.* **2014**, *85*, No. 015119.
(30) Heske, C.; Groh, U.; Fuchs, O.; Weinhardt, L.; Umbach, E.; Schedel-Niedrig, T.; Fischer, C.-H.; Lux-Steiner, M. C.; Zweigart, S.; Niesen, T. P.; Karg, F.; Denlinger, J. D.; Rude, B.; Andrus, C.; Powell, F. Monitoring chemical reactions at a liquid−solid interface: Water on $CuIn(S,Se)_2$ thin film solar cell absorbers. *J. Chem. Phys.* **2003**, *119*, 10467−10470.
(31) Heske, C. Spectroscopic investigation of buried interfaces and liquids with soft X-rays. *Appl. Phys. A* **2004**, *78*, 829−835.
(32) Fuchs, O.; Weinhardt, L.; Blum, M.; Weigand, M.; Umbach, E.; Bär, M.; Heske, C.; Denlinger, J.; Chuang, Y.-D.; McKinney, W.; Hussain, Z.; Gullikson, E.; Jones, M.; Batson, P.; Nelles, B.; Follath, R. High-resolution, high-transmission soft x-ray spectrometer for the study of biological samples. *Rev. Sci. Instrum.* **2009**, *80*, No. 063103.
(33) Qiao, R.; Li, Q.; Zhuo, Z.; Sallis, S.; Fuchs, O.; Blum, M.; Weinhardt, L.; Heske, C.; Pepper, J.; Jones, M.; Brown, A.; Spucces, A.; Chow, K.; Smith, B.; Glans, P.-A.; Chen, Y.; Yan, S.; Pan, F.; Piper, L. F. J.; Denlinger, J.; Guo, J.; Hussain, Z.; Chuang, Y.-D.; Yang, W. High-efficiency in situ resonant inelastic x-ray scattering (iRIXS) endstation at the Advanced Light Source. *Rev. Sci. Instrum.* **2017**, *88*, No. 033106.
(34) Fouda, A. E. A.; Seitz, L. C.; Hauschild, D.; Blum, M.; Yang, W.; Heske, C.; Weinhardt, L.; Besley, N. A. Observation of Double Excitations in the Resonant Inelastic X-ray Scattering of Nitric Oxide. *JPCL* **2020**, *11*, 7476−7482.
(35) Werme, L. O.; Grennberg, B.; Nordgren, J.; Nordling, C.; Siegbahn, K. Fine Structure in the X-ray Emission Spectrum of N_2, Compared with Electron Spectroscopy. *Nature* **1973**, *242*, 453−455.
(36) Werme, L. O.; Grennberg, B.; Nordgren, J.; Nordling, C.; Siegbahn, K. Observation of Vibrational Fine Structure in X-Ray Emission Lines. *Phys. Rev. Lett.* **1973**, *30*, 523−524.
(37) Nordgren, J.; Ågren, H.; Selander, L.; Nordling, C.; Siegbahn, K. Electron Spectroscopy and Ultra-soft X-ray Emission of Free Molecules. *Phys. Scr.* **1977**, *16*, 280−284.
(38) Ågren, H.; Selander, L.; Nordgren, J.; Nordling, C.; Siegbahn, K.; Müller, J. X-ray spectra and core hole energy curves of some diatomic molecules. *Chem. Phys.* **1979**, *37*, 161−171.
(39) Glans, P.; Skytt, P.; Gunnelin, K.; Guo, J. H.; Nordgren, J. Selectively excited X-ray emission spectra of N_2. *J. Electron Spectrosc. Relat. Phenom.* **1996**, *82*, 193−201.
(40) Nordgren, J.; Agren, H.; Werme, L. O.; Nordling, C.; Siegbahn, K. X-ray emission spectra of NH_3 and N_2O. *J. Phys. B: At. Mol. Phys.* **1976**, *9*, 295−302.
(41) Weinhardt, L.; Weigand, M.; Fuchs, O.; Bär, M.; Blum, M.; Denlinger, J. D.; Yang, W.; Umbach, E.; Heske, C. Nuclear dynamics in the core-excited state of aqueous ammonia probed by resonant inelastic soft x-ray scattering. *Phys. Rev. B* **2011**, *84*, 104202.
(42) Weinhardt, L.; Ertan, E.; Iannuzzi, M.; Weigand, M.; Fuchs, O.; Bär, M.; Blum, M.; Denlinger, J. D.; Yang, W.; Umbach, E.; Odelius, M.; Heske, C. Probing hydrogen bonding orbitals: resonant inelastic

https://doi.org/10.1021/acs.jpcc.2c04736
J. Phys. Chem. C 2022, 126, 20998−21009

soft X-ray scattering of aqueous NH_3. *Phys. Chem. Chem. Phys.* **2015**, *17*, 27145−27153.
(43) Meyer, F.; Blum, M.; Benkert, A.; Hauschild, D.; Jeyachandran, Y. L.; Wilks, R. G.; Yang, W.; Bär, M.; Heske, C.; Reinert, F.; Zharnikov, M.; Weinhardt, L. X-ray Emission Spectroscopy of Proteinogenic Amino Acids at All Relevant Absorption Edges. *JPCB* **2017**, *121*, 6549−6556.
(44) Weinhardt, L.; Benkert, A.; Meyer, F.; Blum, M.; Hauschild, D.; Wilks, R. G.; Bär, M.; Yang, W.; Zharnikov, M.; Reinert, F.; Heske, C. Local electronic structure of the peptide bond probed by resonant inelastic soft X-ray scattering. *Phys. Chem. Chem. Phys.* **2019**, *21*, 13207−13214.
(45) Niwa, M.; Katada, N. Measurements of acidic property of zeolites by temperature programmed desorption of ammonia. *Catal. Surv. Asia* **1997**, *1*, 215−226.
(46) Günter, T. *Katalytische NO_x-Entfernung aus mobilen Abgasen an kleinporigen Zeolithen*. Karlsruher Institut für Technologie (KIT), 2016.
(47) Weinhardt, L.; Steininger, R.; Kreikemeyer-Lorenzo, D.; Mangold, S.; Hauschild, D.; Batchelor, D.; Spangenberg, T.; Heske, C. X-SPEC: A 70 eV to 15 keV undulator beamline for X-ray and electron spectroscopies. *J. Synchrotron Radiat.* **2021**, *28*, 609−617.
(48) Zhang, R.; McEwen, J.-S.; Kollár, M.; Gao, F.; Wang, Y.; Szanyi, J.; Peden, C. H. F. NO Chemisorption on Cu/SSZ-13: A Comparative Study from Infrared Spectroscopy and DFT Calculations. *ACS Catal.* **2014**, *4*, 4093−4105.
(49) Negri, C.; Martini, A.; Deplano, G.; Lomachenko, K. A.; Janssens, T. V. W.; Borfecchia, E.; Berlier, G.; Bordiga, S. Investigating the role of Cu-oxo species in Cu-nitrate formation over Cu-CHA catalysts. *Phys. Chem. Chem. Phys.* **2021**, *23*, 18322−18337.
(50) Li, Y.; Hall, W. K. Catalytic decomposition of nitric oxide over Cu-zeolites. *J. Catal.* **1991**, *129*, 202−215.
(51) Stichler, M.; Keller, C.; Heske, C.; Staufer, M.; Birkenheuer, U.; Rösch, N.; Wurth, W.; Menzel, D. X-ray emission spectroscopy of NO adsorbates on Ru(001). *Surf. Sci.* **2000**, *448*, 164−178.
(52) Staufer, M.; Birkenheuer, U.; Belling, T.; Nörtemann, F.; Rösch, N.; Stichler, M.; Keller, C.; Wurth, W.; Menzel, D.; Pettersson, L. G. M.; Föhlisch, A.; Nilsson, A. Interpretation of x-ray emission spectra: NO adsorbed on Ru(001). *J. Chem. Phys.* **1999**, *111*, 4704−4713.
(53) Rubensson, J. E.; Petersson, L.; Wassdahl, N.; Bäckström, M.; Nordgren, J.; Kvalheim, O. M.; Manne, R. Radiative decay of multiply excited core hole states in H_2O. *J. Chem. Phys.* **1985**, *82*, 4486−4491.
(54) Moya-Cancino, J. G.; Honkanen, A.-P.; van der Eerden, A. M. J.; Oord, R.; Monai, M.; ten Have, I.; Sahle, C. J.; Meirer, F.; Weckhuysen, B. M.; de Groot, F. M. F.; Huotari, S. In Situ X-ray Raman Scattering Spectroscopy of the Formation of Cobalt Carbides in a Co/TiO_2 Fischer−Tropsch Synthesis Catalyst. *ACS Catal.* **2021**, *11*, 809−819.

https://doi.org/10.1021/acs.jpcc.2c04736
J. Phys. Chem. C 2022, 126, 20998−21009